LAWRENCE
LIVERMORE
NATIONAL
LABORATORY

UCRL-TR-209674

Final Report 02-ERD-033: Rapid Resolidification of Metals using Dynamic Compression

F. H. Streitz, J. H. Nguyen, D. Orlikowski, R. Minich, J. A. Moriarty, N. C. Holmes

February 14, 2005

This work was performed under the auspices of the U.S. Department of Energy by University of California, Lawrence Livermore National Laboratory under Contract W-7405-Eng-48.

FINAL REPORT 02-ERD-033:
Rapid Resolidification of Metals using Dynamic Compression

F.H. Streitz, J.H. Nguyen, D. Orlikowski, R. Minich, J.A. Moriarty, N.C. Holmes

Project Description

The purpose of this project is to develop a greater understanding of the kinetics involved during a liquid-solid phase transition occuring at high pressure and temperature. Kinetic limitations are known to play a large role in the dynamics of solidification at low temperatures, determining, e.g., whether a material crystallizes upon freezing or becomes an amorphous solid. The role of kinetics is not at all understood in transitions at high temperature when extreme pressures are involved. In order to investigate time scales during a dynamic compression experiment we needed to create an ability to alter the length of time spent by the sample in the transition region.

Traditionally, the extreme high-pressure phase diagram is studied through a few static and dynamic techniques: static compression involving diamond anvil cells (DAC) [1], shock compression [2, 3], and quasi-isentropic compression [4, 5, 6, 7, 8, 9, 10]. Static DAC experiments explore equilibrium material properties along an isotherm or an isobar [1]. Dynamic material properties can be explored with shock compression [2, 3], probing single states on the Hugoniot, or with quasi-isentropic compression [4, 5, 6, 7, 8, 9, 10]. In the case of shocks, pressures variation typically

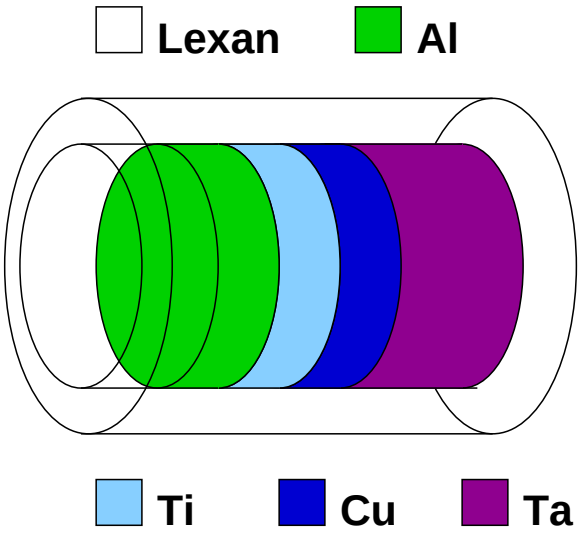

Figure 1: Schematic of earliest bullet design comprised of physically distinct layers of materials with various shock impedence values.

occurs on a sub-nanosecond time scale or faster [11]. Previous quasi-isentropic techniques have yielded pressure ramps on the 10-100 nanosecond time-scale for samples that are several hundred microns thick [4, 5, 6, 7]. In order to understand kinetic effects at high temperatures and high pressures, we need to span a large dynamic range (strain rates, relaxation times, etc.) as well as control the thermodynamic path that the material experiences. Compression rates, for instance, need to bridge those of static experiments (seconds to hours) and those of the Z-accelerator ($10^6 s^{-1}$) [4] or even laser ablation techniques ($10^6 s^{-1}$ to $10^8 s^{-1}$) [7]. Here, we present a new technique that both extends the compression time to several microseconds and makes accessible states beyond the principal Hugoniot and isentrope. The strain rate in these quasi-isentropic compression experiments vary from $10^4 - 10^6 \mathrm{s}^{-1}$, effectively bridging the gap between static compression and previous quasi-isentropic compression techniques [4, 7].

The primary deliverable associated with this LDRD-ER is the creation a new experimental capability for the lab: the ability to control pressure and temperature loading rates in a dynamic compression experiment by using functionally graded impactors in the light gas gun facility. The new capability will enable dynamic experiments exploring a broader area of pressure and temperature phase space, ultimately enabling further experiments on the kinetics of phase transitions at high temperature and pressure. Using our unique arbitrary-density graded impactors, scientists can now investigate various aspects of the solidification phase transition including (a) time scale, (b) loading rate dependence and (c) sample size effects.

Activities

Development of graded density impactor (GDI)

We have made substantial progress in the development of layered impactors for the creation of a near isentropic compression. Our original design consisted of discrete layers of various metals arranged with increasing density along the direction of shock propagation, as shown in Figure 1 This approach, conceptually similar in nature to "ring-up" experiments routinely performed in dynamic compression experiments, was demonstrated during the first year of the project. Figure 2 displays an example VISAR trace from an experiment using such a layered bullet - demonstrating the multiple small shocks which appeared in sample as a result of impact. The original design evolved rapidly into one utilzing a more favorable approach that provides much smoother pressure ramps by using powder metallurgy. These second generation bullets are manufactured by mixing Al and W powders in fixed proportions and then assembling fine layers of the resulting powders(each 200 ± 20 μm thick) in order

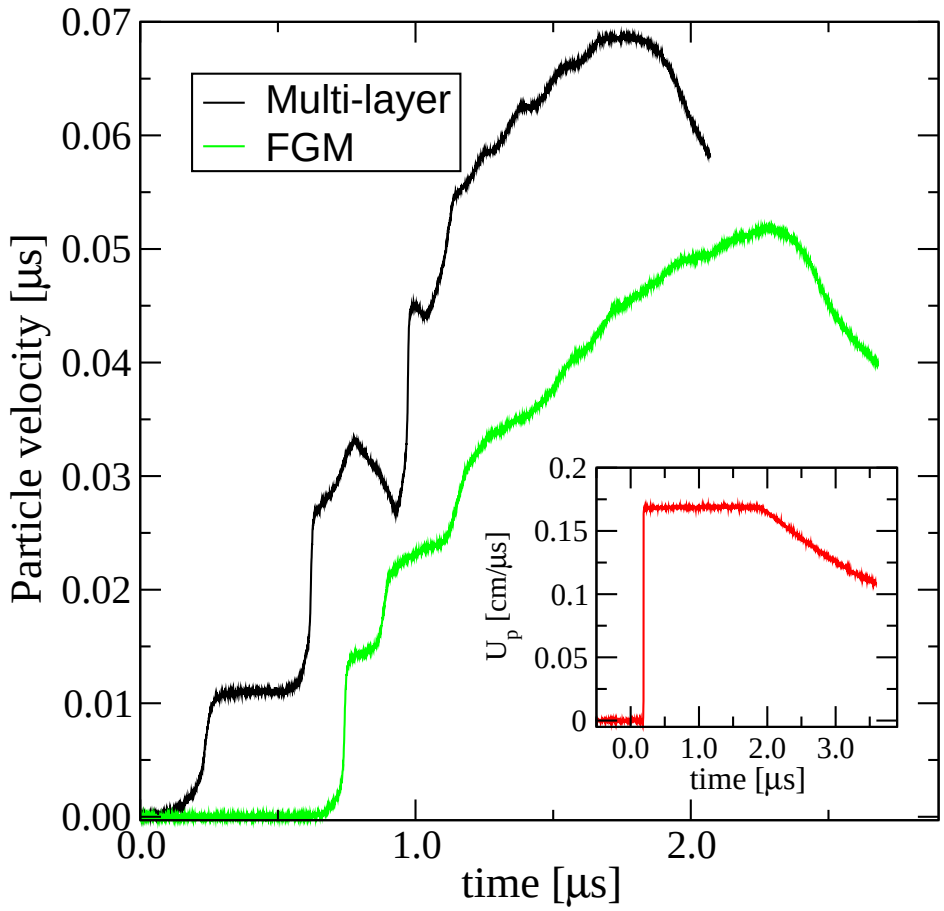

Figure 2: Particle velocity vs. time taken from a VISAR trace of an older, Multi-layered impactor and a FGM impactor. The inset displays the response of a single flyer plate producing a simple shock.

of increasing density (i.e., Al powder, followed by 90% Al/10% W, followed by 80% Al/20% W, etc...) The final assembly is then infused with a resin epoxy, producing a metal/resin composite bullet with a density gradient ranging from a minimum of about 1.2 g/cc to a maximum of around 8.0 g/cc. The progressively higher shock impedance values for the layers in the impactor modulate the pressure increase caused by its impact, as before. Figure 2 compares a resulting particle velocity (or pressure) trace vs. time for our Graded Density Impactor (GDI) and our original multi-layered design, as well a profile from a simple shock. The GDI is seen to produce quite smooth

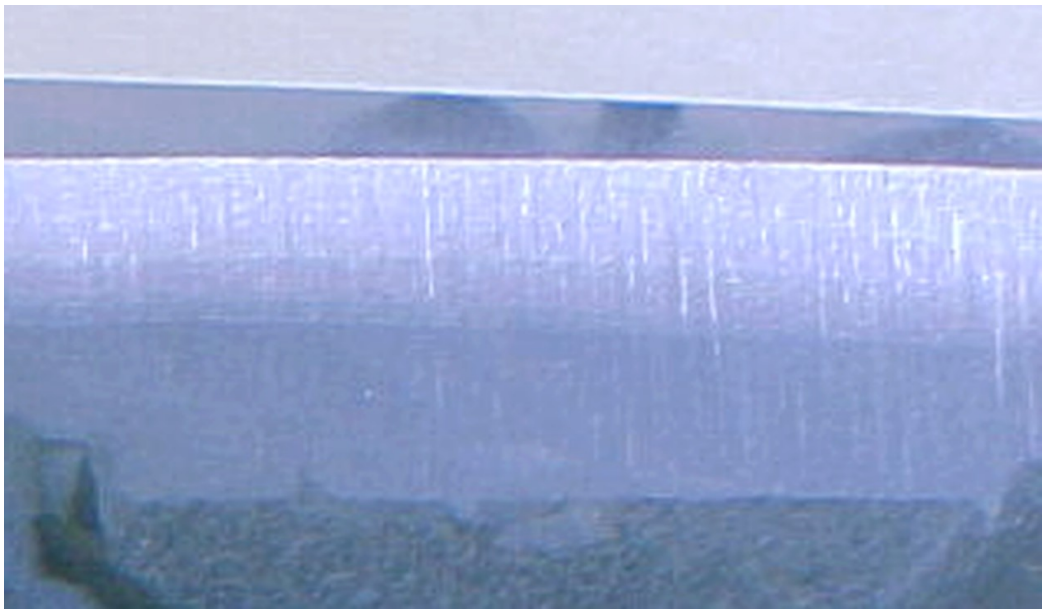

Figure 3: Cross-sectional image of a GDI demonstrating the variation in density from pure Al to pure W a 3mm thickness. This GDI was made by sintering an assembly of metal powder layers.

pressure ramps over time scale as long as μs, approximately 3-4 orders of magnitude slower than the time scale of a pure shock.

The introduction of mixtures of powdered metals as a means of generating a functionally graded material for use as an impactor was deemed sufficiently novel that the laboratory is seeking patent protection on its use[1].

The low density region of the GDI manufactured using this technique was found to still cause a small shock on impact, hampering efforts to produce a pure isentropic compression. Working closely with scientists at Sandia National Laboratory (in Livermore) we began investigating the use of foam particles as a binder for the metallic powders, replacing the resin (which had a minimum density of approx. 1.2 g/cc). Introducing Expancel foam[2], which is a hollow expandable assembly of polymeric microballoons (comprised of copolymers of polyacrylonitrile and polymethacrylonitrile, with an average un-expanded diameter of 10-15 μm) allowed us to produce final layers with densities as low as several hundredths of a g/cc. In practice, however, we found that these extremely light layers were difficult to process and could not survive the process of being fired as an impactor in the light gas gun. Thus, we limited the lowest densities to about 0.1 g/cc in order to maintain the integrity of the impactor during

[1]The invention is fully described in LLNL ROI #IL-11172

[2]see Sandia Report SAND2000-8217

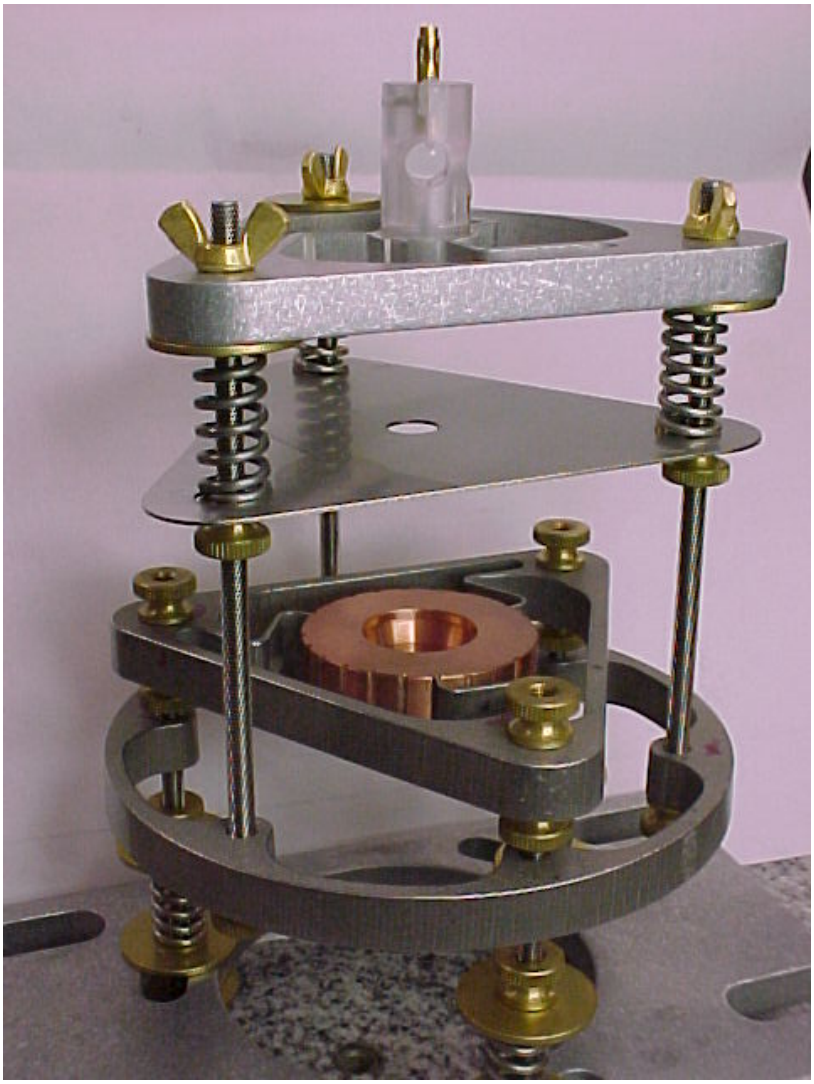

Figure 4: Improved target design, showing target assembly, mounting hardware and heat shields.

firing (where acceleration can be 80,000 m/s^2).

In order to attain higher final pressures, we created layers by mixing appropriate percentages of pure Al and W and then sintering the resulting structure. This procedure produced layer densities no longer limited by the use of a resin matrix as a binder. Sintering at modest temperature and pressure allowed the creation of nearly fully dense graded materials, with densities ranging from that of pure Al (2.7 g/cc) to that of pure W (15 g/cc). (See Figure 3.) By assembling the appropriate layers created using all three techniques (Expancel/metal powder layers, resin/metal powder layers, and pure sintered metal powders) we can create GDI with density ranging

from 0.1 g/cc to 15 g/cc.

Non-linearity in the response of materials to compression waves and complex wave interactions occurring in the sample preclude simple translation of impedance profile to compression path. (i.e., a linear impedance profile does not generate a linear pressure profile.) To calculate the impedance profile necessary to produce a specific desired pressure pulse, we perform extensive hydrodynamic simulations of impact, starting with an initial guess for the impedance profile and iterating until we have produced the desired compression path. The 1D (in the direction of impact) hydrodynamic simulations utilize analytical equations of state (EOS) and incorporate strength effects through Steinberg-Guinan model [12]. This necessitates a parallel effort to determine the EOS and strength parameters for each unique layer appearing in the impactor, a process which is accomplished by comparing the results of the simulations with experiments conducted on known samples, such as Cu and Al.

Design of targets for dynamics experiments on liquids

We investigated isentropic compression on two different liquids: molten Bi and water. Bismuth is a material ideally suited for this study due to its low ambient melting point (551 K) and the relatively low pressure at which the liquid isentrope crosses the melt curve. The low melt temperature enabled us to successfully employ simple resistive heating methods in order to melt the sample. The entire experiment could be easily performed on the smaller gas gun that is limited to about 2km/s projectile velocity, as this velicity was sufficient to attain the low solidification pressure. Of paramount concern during the design was preventing the loss of liquid bismuth into the vacuum of the target chamber after melt. After early attempts involving adhesives proved futile, the target design was substantially improved by incorporating a copper bushing surrounding the window (LiF or sapphire) and enclosed by a pair of copper ferrules engineered to crimp into the bushing, sealing the window/bushing against the loss of melted Bi. By avoiding the use of adhesives in the target we enable the use of this design to high temperatures limited only by the melting points of the window and/or optical assemblies. This target design, shown in Figure 4, was utilized for our early Bi shots. One feature of the target design was the presence of a reservoir above the actual sample, to accomodate the densification of Bi under melt. We found that in practice the Bi did not always flow from the reservoir to the sample, causing instead the liquid Bi to pull away from the LiF window creating voids. Upon identifying this difficulty, we re-designed the target to include a small piston mounted with a light spring, so that the liquid Bi is gently forced to maintain intimate contact with the window. This redesign was used for the later molten Bi shots described below.

The target design for water was substantially simpler, as we needed to concern

ourselves with neither heating nor contraction of the sample. The final design was constructed out of aluminum and includes a feature enabling us to load the sample with water only moments prior to the shot, in order to minimize the time during which the distilled and degassed water was in contact with its surrounding.

Atomic scale simulations of resolidification

One of the goals of this project was to model the solidification of Bi under isentropic compression using molecular dynamics techniques that were being developed as part of the ASCI program. Despite our efforts, we proved unable to create a viable interatomic potential to describe the interactions between the Bi atoms, severely impacting our ability to model the solidification of bismuth. We successfully modeled the solidification of a simpler metal (namely, Ta) using molecular dynamics techniques as part of the Rapid Resolidification project under the ASCI program. Those simulations were not funded as part of this LDRD and are described elsewhere[15].

Technical Accomplishments

The primary goals of this project were the creation of an isentropic compression capability for the Livermore gas guns and the investigation (using this new ability) of pressure-induced liquid-solid phase transitions in metals. The project succeeding in attaining both of these goals, as described below.

Arbitrary compression profiles with GDI

We describe here our method for creating a dynamic compression pulse that allows an unprecedented level of experimental control on the form and time scale of the pressure

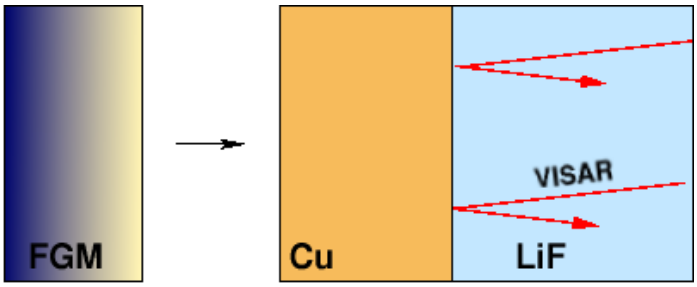

Figure 5: A functionally graded density impactor (3-8 mm thick) is typically accelerated up to 4 km/s in these experiments. It impacts a Cu sample tamped with a LiF window. The Cu sample is typically several mm thick, and flat to better than 5 μm, while the LiF window is typically 10 mm thick. A VISAR probe is used to measure the velocity at the sample/LiF interface.

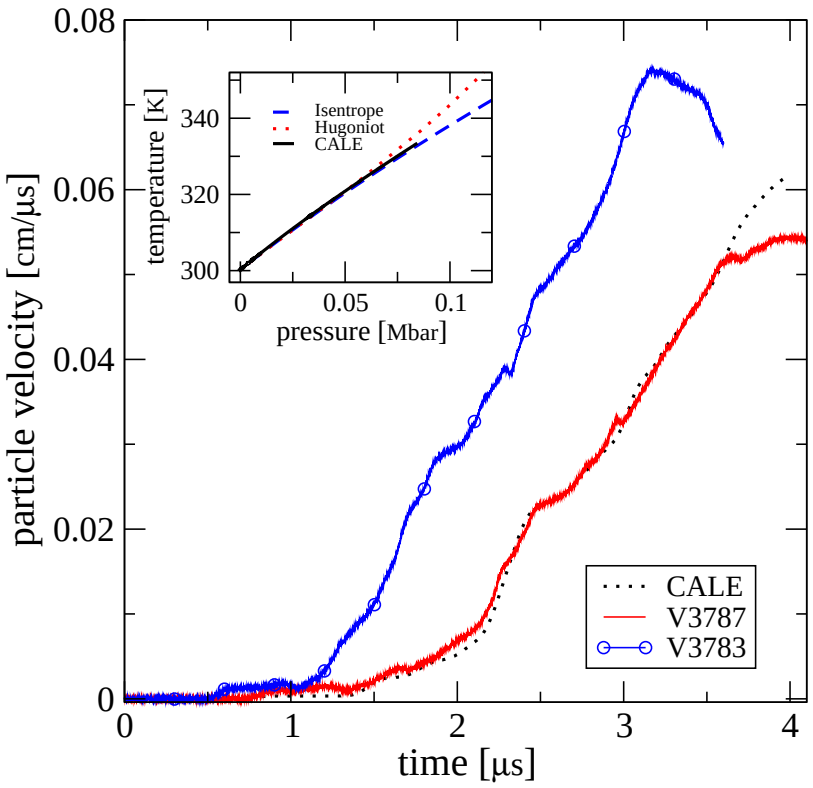

Figure 6: Typical compression light-gas gun experiment (impactor velocity 1.0 km/s (V3787) and 1.2 km/s (V3783)) is shown (solid-lines). A hydrodynamic calculation (CALE), that models the impactor composition, simulates the experiment in one dimension. The deviation of the experiment from calculation at 0.05 cm/μs is due to rarefraction (release) waves from the side of the Cu-target. Inset: a comparison is made between the thermodynamic path of the modeled experiment, Hugoniot, and the isentrope for Cu. The calculation is within 0.2 % (numerical error) of the isentrope and is $\approx$1 % of the Hugoniot at the highest obtained pressure. The strain is 6%.

profile. The method allows complete flexibility in designing into the pressure profile elements of shock, isentropic compression, controlled release and static pressure, with the resulting pulse occurring on time scales ranging from 10's of ns to several μs. This approach not only removes the constraint of specific thermodynamic path, but also helps bridge the gap in loading rate between a static and shock compression experiment.

The ability to apply a nearly arbitrary shaped pressure pulse to a sample rests on our ability to create a correspondingly arbitrary shock impedance[3] profile in the

[3]impedance = $c\rho_\circ$, where c is the sound speed and $\rho_\circ$ the density

impactor. An increasing impedance profile in the impactor imparts a compression, while a decreasing impedance profile translates to a controlled release of pressure (or rarefaction) in the sample. Abrupt increases in impedance can be used to generate a shocks in the sample. Our impactors are constructed by assembling a sequence of fine layers ($\approx 200 \pm 20\,\mu$m thick) each with a specific shock impedance value. The individual layers are themselves composed of Al and W powders ($\leq 5\mu m$ in size), mixed in the appropriate proportions to produce the desired impedance. Sintering the powders yields the highest densities (2.7 g/cc to 15 g/cc). We create layers with lower densities by embedding the powders in a resin matrix (final densities of 1.2 g/cc to 8 g/cc) or a foam matrix (densities of 0.01 g/cc to 2.7 g/cc). In practice, we restrict the lowest densities to about 0.1 g/cc in order to maintain the integrity of the impactor during firing (where acceleration can be as high as 8000 g). By employing any or all of these techniques as needed, we can produce impactors with densities ranging from 0.1 g/cc to 15 g/cc over a space of several millimeters.

Non-linearity in the response of materials to compression waves and complex wave interactions occurring in the sample preclude simple translation of impedance profile to compression path. (i.e., a linear impedance profile does not generate a linear pressure profile.) To calculate the impedance profile necessary to produce a specific desired pressure pulse, we perform extensive hydrodynamic simulations of impact, starting with an initial guess for the impedance profile and iterating until we have

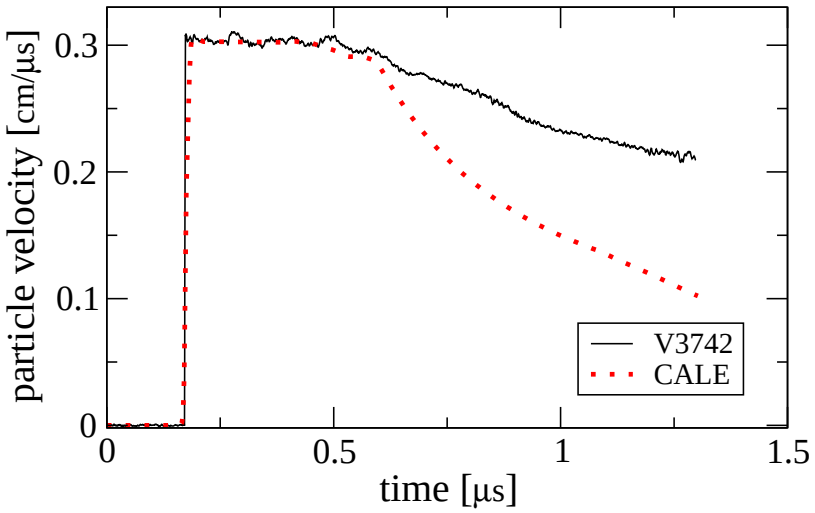

Figure 7: The U_p record (Cu/LiF interface, solid-line) is shown for a controlled rarefraction (release) wave at different strain-rate as compared with the simulated rarefraction wave (dotted-line) that originates from the free-surface of the back-end of a single-density impactor, which is typical in standard shock experiments.

produced the desired compression path. The 1D (in the direction of impact) hydrodynamic simulations utilize analytical equations of state (EOS) and incorporate strength effects through Steinberg-Guinan model [12]. This necessitates a parallel effort to determine the EOS and strength parameters for each unique layer appearing in the impactor, a process which is accomplished by comparing the results of the simulations with experiments conducted on known samples, such as Cu and Al.

For the light-gas gun experiments presented here, these monotonic or non-monotonic pressure profiles are produced by creating a similar profile in the density of the impactor. The designed impactors are composed of functionally graded material (FGM), whose density (and hence shock impedance) profile can be specifically varied from less than 0.1 g/cc to more than 15 g/cc. Monotonically increasing density profile impactors are used to generate quasi-isentropic compression in the target samples. The initial weak shocks observed in previous techniques [8, 9, 10] are reduced below the elastic limit with an initial density ($\leq$ 0.1g/cc) in the impactors. High densities ($\geq$15 g/cc), on the other hand, help us achieve megabar pressures in the samples. Variations in impactor profile and impactor velocity can be exploited to attain experimental time-scales from tens of nanoseconds to a few microseconds, which is an order of magnitude slower than Z-accelerator [4, 5, 6] and laser ablation [7] experiments.

We have demonstrated the application of these graded density impactors (GDI) by performing a series of experiments on Cu at the two-stage light gas gun. The impactors are launched at at velocities between 1 and 4.5 km/s towards the Cu target (typically a disk several mm thick and flat to better than 5μm, tamped with a 10 mm thick single crystal of LiF), as shown in Figure 5. (We have successfully fired a low density GDI as high as 6 km/s). A velocity interferometer is used to measure the particle velocity U_p at the Cu-LiF interface [13], and hydrodynamic simulations of the experiment are performed using the previously developed EOS's for the bullet in order to infer the pressure and temperature path of the sample during compression.

Two representative isentropic compression results obtained from impact of a simple GDI (with monotonic impedance profile) onto Cu are shown in Figure 6, which displays U_p at the Cu-LiF interface as a function of time. The particle velocities are seen to rise smoothly, with no evidence of shock, for a period of 2 to 3 μs, reaching peak velocities of 0.073 and 0.05 cm/μs. In the inset on Fig.6 we show the path through phase space taken by the Cu sample during the experiment, as predicted by hydrodynamic simulation. The calculated path agrees to better then 0.2% with the isentrope, while the calculated temperature of the sample at peak pressure of 70 GPa is already 1% lower than that on the Hugoniot. The nearly linear increase in particle velocities seen in Fig. 6 is evidence of a nearly constant strain rate during the experiment. (The slight deviations from a linear increase in particle velocity represent

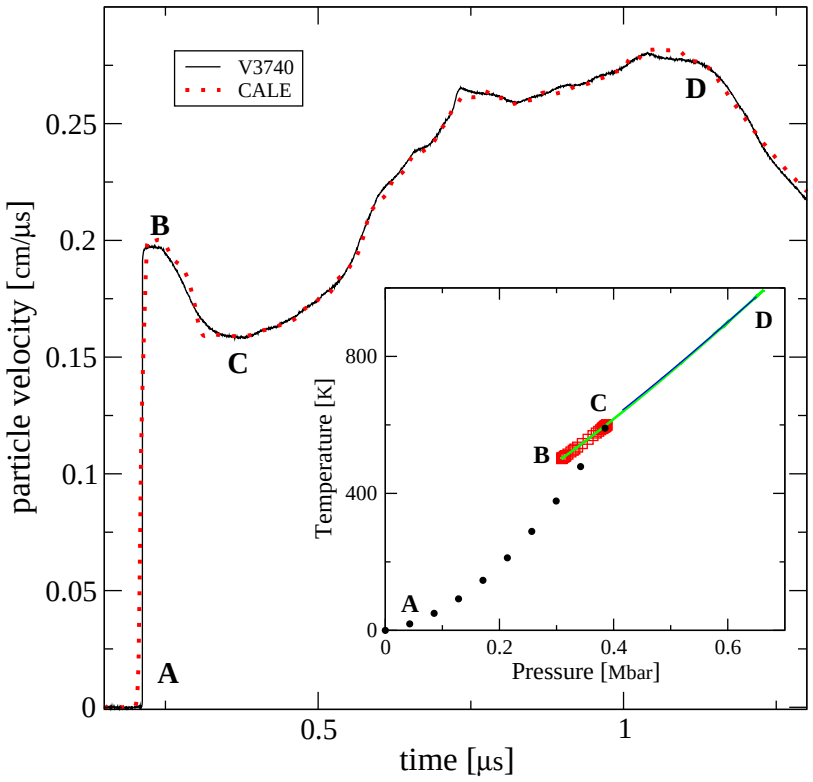

Figure 8: A VISAR trace (Cu/LiF interface) shows a Cu system that is shock compressed (A-B), released (B-C), quasi-isentropically compressed (C-D) and finally released. The hydro-simulation (dotted-line) overlays the experimental VISAR trace. (Inset) From simulation, the corresponding path in the temperature and pressure (T-P) plane. Dotted line in the inset denotes the shock Hugoniot.

small variations in strain rate along the isentrope, and do not induce movement off of the isentrope.) Using the results of hydrodynamic simulations, we estimate the strain rate to average $2-3\times10^{4}\mathrm{s}^{-1}$ for these shots. Strain rates this low (an order of magnitude lower than what has been presented using other quasi-isentropic compression techniques [4, 5, 6, 7]) are below the phonon drag regime[14], and have been shown in atomistic models to be sufficiently slow to access the equilibrium thermodynamic phase diagram [15]. Hence, using GDI we have effectively bridged the time-scale gap between static and dynamic compression.

The ability to control the time scale of the experiment extends to release, as well. By creating a GDI with a constant initial impedance followed by a slowly *decreasing* impedance, we can control the rate of release of pressure, as demonstrated in Figure 7. The particle velocity in the release (rarefraction) wave for this experiment decreases

a factor of three slower than if release had occurred from a single density impactor. Such impactors could be used to mimic in one dimension the release which occurs following an explosion [16].

The utility of the use of a GDI lies not only in the ability to control the time scale of the compression or rarefaction, but in the ability to produce a nearly arbitrary pressure profile (thermodynamic path) in a sample. Complete control of the density (impedance) profile in the impactor allows one to juxtapose at will regions which will produce compressions, rarefactions, shocks, or constant pressure in the sample. By applying these pressure producing regions in a specified sequence, one can move a sample through complex paths in phase space.

We demonstrated one such complex path in Figure 8, which depicts the particle velocity measured at a Cu/LiF interface. For this experiment, the impactor was comprised of a uniform, high density layer followed by a monotonically increasing

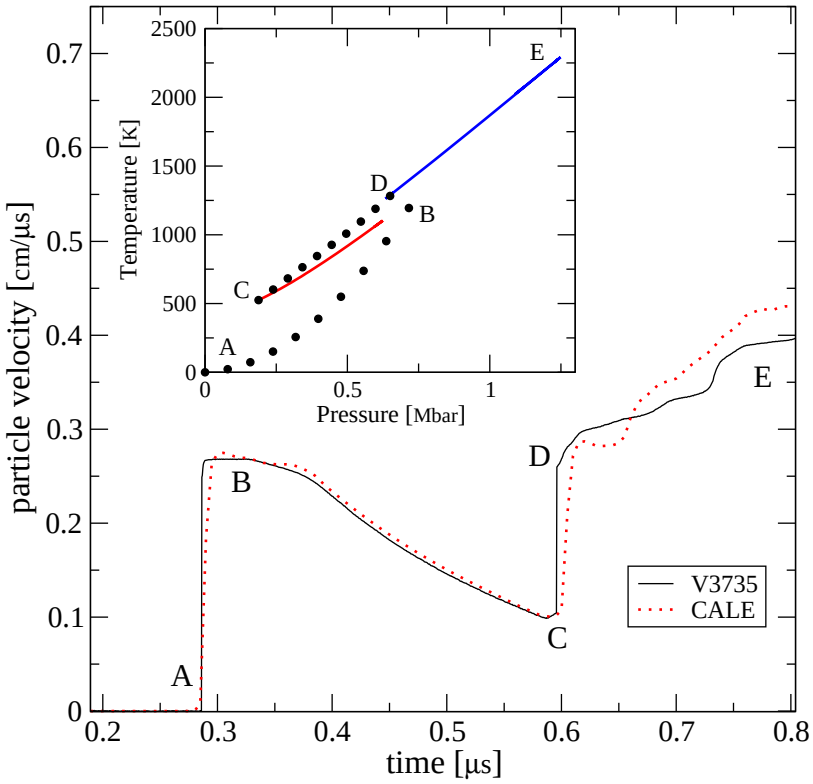

Figure 9: A variation of figure 8 is shown, where the VISAR trace (Cu/LiF interface) and hydro-simulation (dotted line) are given. (Inset) the corresponding T-P path from the simulation with the Hugoniots (dotted lines). The system is shock compressed (A-B), released (B-C), re-shocked (C-D), and quasi-isentropically compressed (D-E).

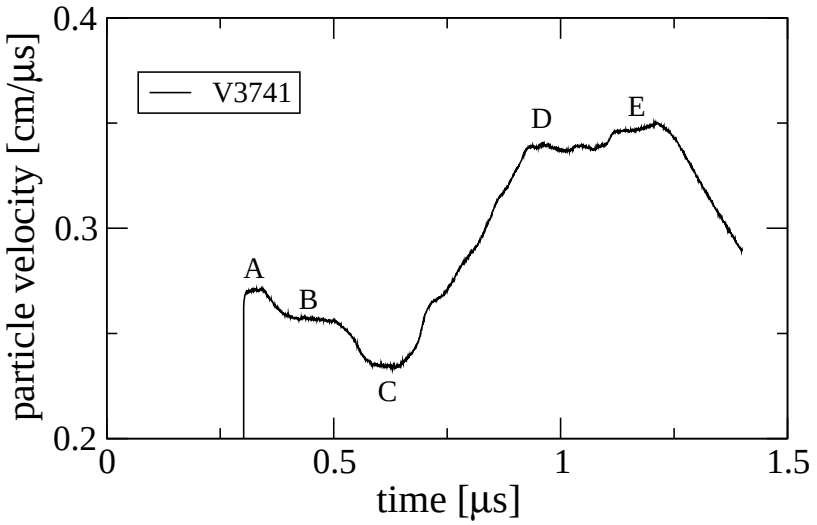

Figure 10: A VISAR trace produced through a complex density arrangement in the impactor shows that the Cu system was controlled to and held at several thermodynamic states via a shock to point (A), controlled releases (A-B and B-C), and quasi-compression (C-D and D-E).

graded density layer. The thermodynamic path taken by the Cu involves a shock to a state on the Hugoniot, followed by traversal of the isentrope on both decompression and compression (see inset Fig. 8). The pressure-temperature (P-T) points to which the sample can be initially shocked, released and finally compressed (points B, C, and D, respectively, in Fig. 8, inset), as well as the relevant strain rates, can be chosen in advance by the experimentalist and designed into the GDI. With proper consideration of the GDI profile and the impactor velocity, one can access a broad region of phase space which was previously inaccessible. Indeed, the high P-T isentrope (BCD in Fig. 8) explored in this demonstration shot could not have been attained from ambient conditions using any conventional technique [2, 3, 4, 5, 6, 7, 8, 9, 10].

The simplest demonstration of pressure and time control were carried out with a reversed impactor, i.e., a simple reversal of the density profile used in figure 6. The particle velocity of the release (rarefraction) wave decreases much slower than if released from a single density impactor (Fig. 7), corresponding to a slower strain-rate by a factor of 3 ($\dot{\epsilon} \approx 5 \times 10^5\, s^{-1}$). Simple modification of this impactor would allow one to dynamically control the pressure, time and, to some extent, the temperature of the sample on pressure release.

An experiment such as this could be designed to investigate melt in shocked-samples on release [17], but at varied rates accessing the phase transition rate.

We can also take the sample through a more complicated thermodynamic path such as a shock to a state on the Hugoniot followed by a traversing of the isentrope,

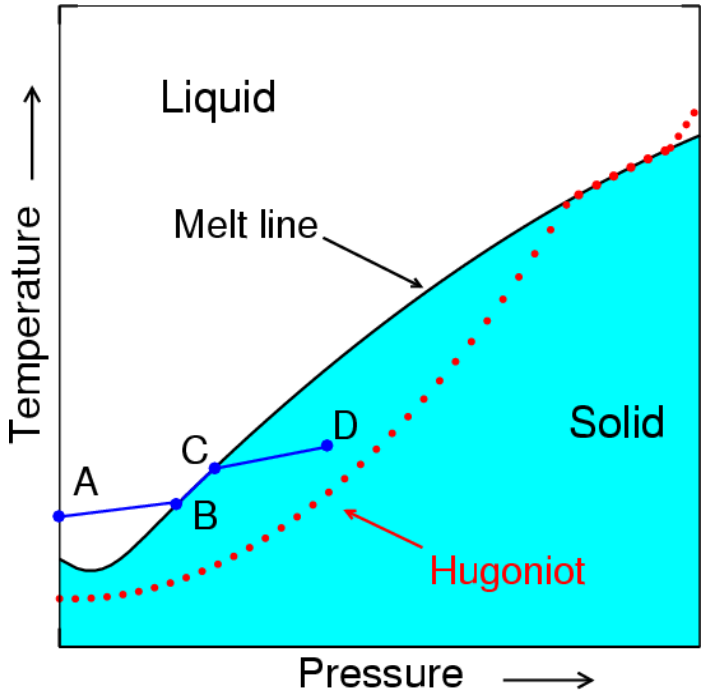

Figure 11: A schematic phase diagram of bismuth with an isentrope (ABCD) sketching the pathway to resolidification: a solid bismuth system is heated and melted to point A; the liquid is then compressed along its isentrope(blue line) to point B; the heat of fusion contained by the system is released as it undergoes a first-order phase transition until C, from which the now solid bismuth is isentropically compressed to its final state at D. The principal Hugoniot (from ambient conditions) indicates approximately the boundary of the phase diagram previously explored (red dotted line). A Hugoniot from point A would never reach the melt line (i.e., a single shock does not cross the Bi melt line) due to the excessive heat generated by a shock.

both on compression and decompression (Fig. 8). The impactor used here has a uniform, high density layer in front of a monotonically increasing graded density layer. The pressure-temperature (P, T) point to which the sample can be initially shocked to, released to, and finally isentropically compressed to (points B, C, and D, respectively, Fig. 8) can be designed into the impactor profile and the impactor velocity. Strain-rate on the isentrope is part of this pre-design. This experiment demonstrates that by properly designing an impactor, we can dynamically access a broad region of phase space which was previously inaccessible. Traversing the high (P, T) isentrope (Fig. 8 inset, BCD path) could not be dynamically achieved with conventional techniques from ambient conditions [2, 3, 4, 5, 6, 7, 8, 9, 10]. Our ability to move beyond the shock Hugoniot and traverse the isentrope both on compression and release made this thermodynamic path possible.

As a result of subsequent increasing density in the FGM, the sample is re-compressed to a peak velocity of $U_p \approx 2.8$ km/s. The shock wave introduces significant entropy in the target, resulting in heating; the state of the Cu jumps from ambient conditions (point A, Fig. 8) to a Hugoniot state (B). From this state, the system releases isentropically, driven by the rarefraction wave. That is, the Cu sample moves continuously along its isentrope between points B-C (see inset Fig. 8). The Cu target is then quasi-isentropically compressed back along the same isentrope (points C-D), passing the initial shock state to reach a peak pressure of 0.65 Mbar. A rarefraction wave from the back of the impactor now releases the sample, causing it to descend the isentrope from point D. The fact that this isentropic release occurs along the same path as the earlier compression is empirical evidence that the previous compression was isentropic.

Additionally, by utilizing the ability to dynamically traverse a nearly identical isentrope on both compression and release, we can now examine the effect of history on material properties. Dynamic phase transitions, for instance, can be investigated for the presence of dynamic hysteresis effect.

Clearly, many other thermodynamic paths are possible. In figure 9, we demonstrated a sequence of thermodynamic states—such as a family of isentropes and shock Hugoniots. In this example, the sample, which is released from a shocked state, is shocked again before being isentropically compressed. It differs from previous example (Fig. 8) in that it allows for continuous exploration of states away from the first isentrope. In some experiments, it may be advantageous to hold the sample at constant pressure to allow for chemical reactions or phase transitions to complete. Such an experiment is shown in Fig. 10, where a much more complex density profile in the impactor was used. In addition to a sequence of shock, releases, and isentropic compression as demonstrated in previous examples, we held the sample at different constant pressures for $\Delta t \approx 0.15 \mu s$. The control of the magnitude and duration of pressure during the experiment can help ensure a well-defined mechanical and thermodynamic state, as well as allow for diagnostic measurements. In this way a system could be studied through multiple phases while allowing time for complete transformation before preceding to the next phase within the experiment.

As in the previous example (Fig. 8), this allows the study of state-dependent strength effects or possible phase boundary shifts due to dynamics.

These are just a few demonstrations of the capability of the functionally graded density impactor in a gas-gun configuration. On the one hand, it can be used to extend the strain-rate of quasi-isentropic compression experiments. This in effect increases the time-scale of the experiments and thickness of the samples. On the other hand, with appropriate pre-planning and by incorporating hydrodynamic simulations,

one can explore complex and previously unattainable thermodynamic paths, greatly expanding access to the high pressure-temperature phase diagram. We were able to achieve this capability by designing a sequence of shock, isentropic compression, release, and static pressure in one dynamic experiment. Using this technique, one can also dynamically probe those features of a phase diagram which have some inherent time dependence, such as phase transitions, or one can investigate the dynamics of material response along various thermodynamic paths. Currently, this FGM impactor is being applied to a study of liquid-solid phase transitions that investigates strain-rate effects, kinetics and possible hysteresis effects, as well as time-scales [18].

Resolidification

Our first application of this method is to resolidify Bi by isentropically compressing a molten sample into a high pressure solid phase. For these experiments, we used three different targets each comprised of a copper vessel, liquid bismuth and a LiF window as shown schematically in Fig. 12. The targets are constructed with solid bismuth in a copper container. To create a liquid sample, the entire assembly is resistively heated to 577 °K (30 °K above the melting point for Bi) for a minimum of fifteen minutes prior to impact, while a surrounding stainless steel armature supporting heat shields and the VISAR probes remained at or near ambient temperatures. Care was taken in preparing the target to contain the liquid bismuth, since densification occurs upon melting at ambient conditions. The occurrence of bulk melting was easily verified by the appearance of at T_m a distinctive plateau in temperature during heating. We initially verified the compression due to the FGM impactor by measuring simultaneously (synchronous to within 20 ns) the particle velocities, which are proportional to pressure, from both a copper and initially liquid bismuth samples as seen in Fig. 13. The particle velocity measured from the Bi/LiF interface indicates a later arrival of the first weak shock, which is consistent with the lower sound speed in liquid Bi, (1.65 km/s *vs.* 3.55 km/s in Cu) [19, 20, 21]. After three weak shocks in the Bi sample, the particle velocity continues to smoothly increase with the applied pressure, exhibiting all the same characteristics seen in the copper trace until approximately 1.2 μs, at which point the slope of the liquid Bi particle velocity flattens while the copper velocity continues to increase, suggesting the onset of the phase transition (point B in Fig. 11). This behavior is similar to that seen with models for solid-solid transitions [23, 24, 25, 26]. As our current hydrodynamic simulations do not include the effects of first order phase transitions, deviations from the model for bismuth (Fig. 13 (c)), but not for copper (fig. 13 (b)) are expected. As the system moves along the melt line, the heat of fusion—normally released to the surrounding medium upon freezing—must be absorbed by the sample, since the

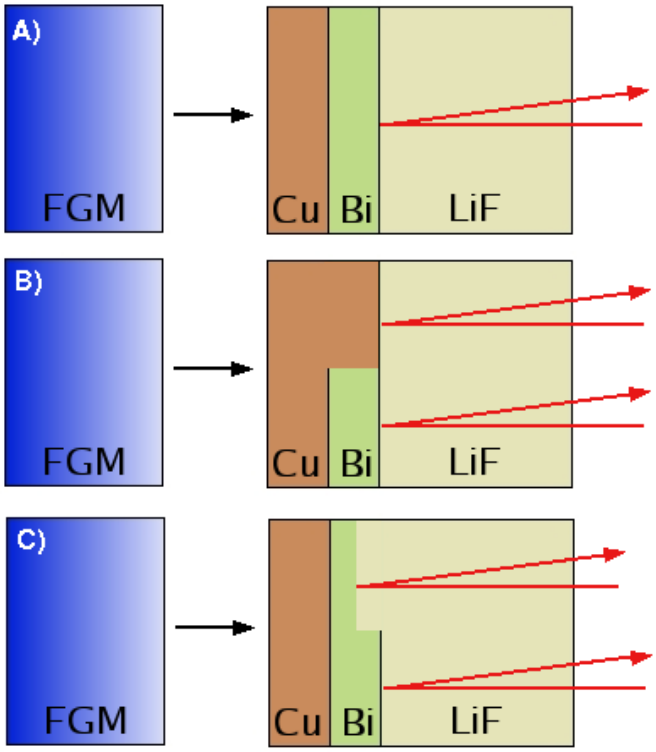

Figure 12: A portrayal of the experiment: a impactor designed with an increasing density (shock impedance) impacts a copper container that holds liquid bismuth. We measured particle velocity U_p at the Bi/LiF and Cu/LiF interface using VISAR, where a single VISAR (setup A) and with two VISARs (setup B and C). The first set of targets (a) was used to measure the particle velocity at the Bi/LiF interface. The dual VISAR target (b) allows simultaneously for the confirmation of the compression due to the impactor in the known copper plate, while observing the liquid Bi sample. Dual VISAR targets of two Bi sample thicknesses (c) are used to reduce error between different shots in order to calculate the Lagrangian sound velocity.

heat transport by phonon modes is too slow to effectively reduce the temperature of the system within the time of the transition. This results in an increase in the sample temperature. With increasing temperature and pressure, the system—now with an growing percentage of solid bismuth—moves along the melt line (from B to C in Fig. 11) until just before 1.5 μs. At this time, the newly solidified Bi sample is driven off the melt curve and begins approaching its final compressed state (point D). This is indicated by a change in particle velocity slope seen in the Bi sample at 1.48 μs, but absent in the Cu trace.

To provide further evidence of resolidification, we compared the release (rarefac-

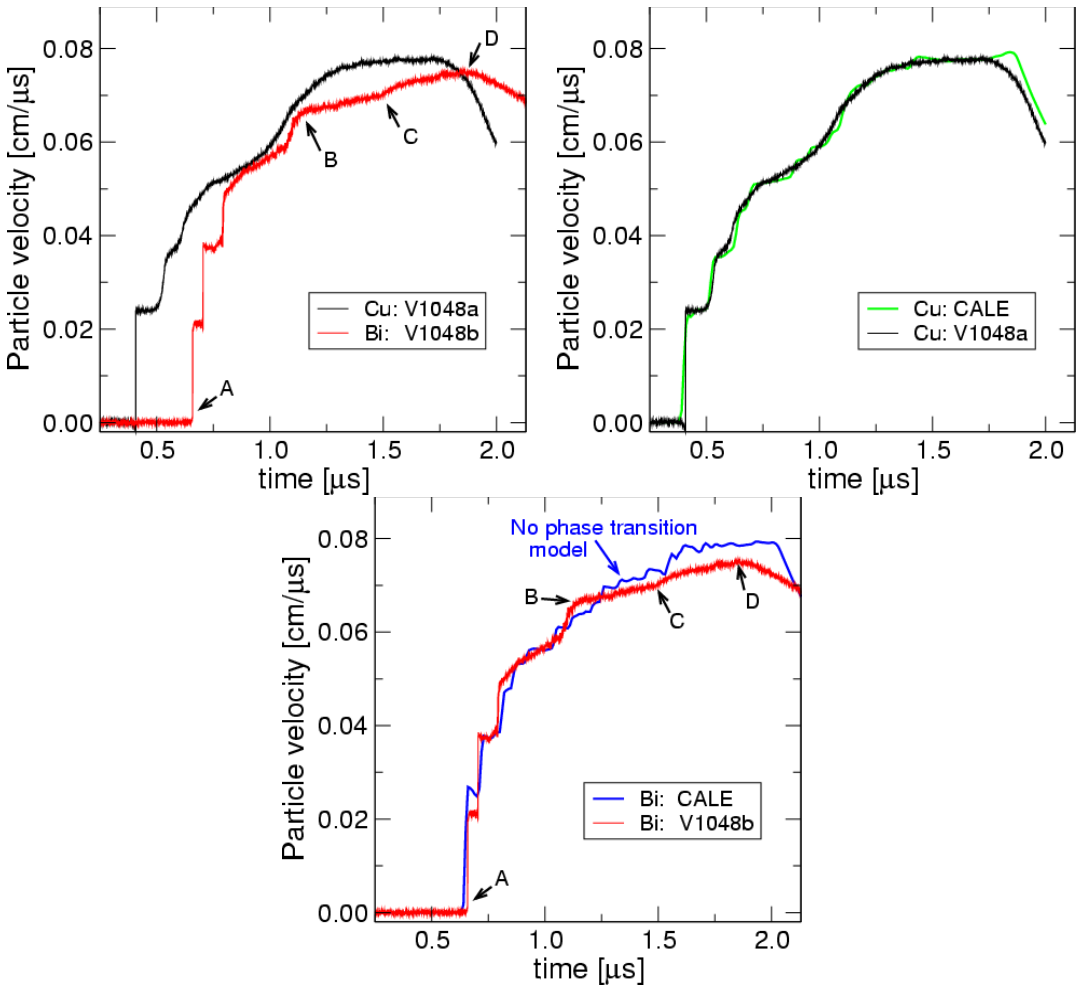

Figure 13: (a) Particle velocities observed simultaneously using the dual VISAR setup (Fig. 12 (b)): data from the Cu/LiF interface VISAR (black) indicates the applied pressure profile, while liquid Bi/LiF interface VISAR (red) indicates the response of the Bi. The ABCD points indicate that correspond to points sketched in Fig. 11. Peak pressure is obtained at point D. The Cu sample is 1.75 mm thick, while the Bi sample is 0.87 mm thick; the impactor velocity is 1.3 km/s. The sudden flattening (B-C) in slope seen in the liquid particle velocity trace near 1.2 μs suggests the solidification transition. In (b) the Cu U_p from (a) is shown in conjunction with the hydrodynamic simulation modeling the impact on the Cu. In (c) the Bi U_p is shown, where the same modeled impactor determined in (b) was used. The hydrodynamic simulation does not contain any phase transitions; therefore, the simulation shows the system's response as if there phase transition did not occur.

tion) wave of figure 13 to the release wave of a solid Bi sample that was shocked to similar pressures. For the shock experiments, we used a simple tantalum or copper impactor with a target comprised of a solid bismuth plate and an attached LiF window. In Figure 14, we display the VISAR traces of the particle velocity at the Bi/LiF interface for three such samples. Sample A was shocked to a solid state on the Hugoniot near point D in Fig. 11. This is similar to the state achieved in our quasi-isentropically compressed and solidified bismuth sample (Fig. 13). Sample B was shocked onto the melt curve (i.e., onto that region of phase space where the Hugoniot and the melt curve coincide). During release, this system follows the melt curve for a short time and then departs from the curve when the sample completely melts. Sample C was shock melted and releases entirely in the liquid phase. Both samples B and C display a sharp reduction of velocity upon release, which could be simulated accurately by modeling the Bi sample as a liquid in hydrodynamic simulations. Sample A, however, displays a gradual reduction in velocity during release, requiring the modeling of strength effects in the solid [12, 27, 28]. By comparing the release measured in the initially liquid Bi sample (Fig. 13) and the releases of samples A, B, and C, we conclude that the isentropically compressed Bi sample is releasing as a solid, suggesting that the liquid bismuth sample had indeed resolidified. These same features of resolidification are evident in experiments performed with differing loading rates and sample thicknesses as well—Fig. 15 depicts the particle velocity traces taken from experiments in which nominally identical impactors were shot at speeds of 1.2 km/s and 1.9 km/s and sample thickness were varied (0.5 mm and 0.98 mm).

Using a different experimental setup, we also empirically calculated the Lagrangian sound speed (in a frame of reference moving with the sample particle) [6] to directly verify the resolidification of the liquid Bi. For this, we simultaneously measured two liquid Bi samples of different thicknesses (setup C in Fig. 12). The results from typical experiments are given in Fig. 16 (Note that the initial shocks, such as seen in Fig. 13, have been systematically removed by the incorporation of a foam matrix into the impactor design.) The small initial shocks in these experiments are at such low particle velocity (low pressure) that the difference between the isentrope and the Hugoniot is negligible. Nevertheless, the quasi-isentropes from each experiment will intersect the melt line at different points due to initial differences in entropy and temperature. Thus, the stronger shock in shot V1171 resulted in a phase transition at higher particle velocity or pressure in comparison to shot V1170 (with a lower initial shock) or to shot V1172 (with no shocks). Figure 17 displays the Lagrangian sound velocity C_L [29] for the particle velocity data of Fig. 16. Sound velocity in the solid phase is expected to be higher than that in the liquid phase at similar pressure

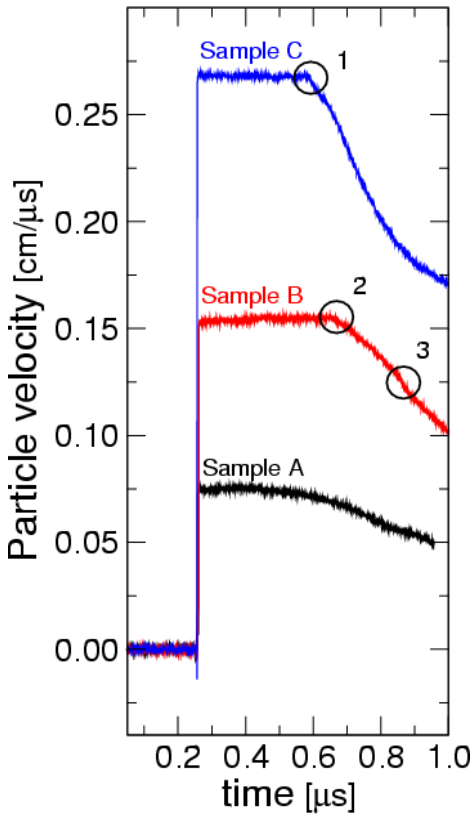

Figure 14: VISAR data recorded from simple shock experiments along the principal Hugoniot of Bi. This is used specifically to compare the strength behaviour, as the system isentropically lowers in particle velocity (pressure), to the isentropically compressed samples. Sample A (Ta impactor velocity 0.93 km/s) is a response through solid Bi beginning at pressures comparable to peak values in the isentropically compression experiments; sample B (Ta impactor velocity 1.9 km/s) is a response beginning from the melt line (region 2) and into liquid indicated by region 3; sample C (Cu impactor velocity 2.1 km/s) is shocked completely into the liquid Bi phase without any strength response (region 1). Pressures obtained through hydrodynamic simulations are: P = 0.13 Mbar for sample A, P = 0.29 Mbar for sample B, P = 0.62 Mbar for sample C. The hydrodynamic simulations of these shocked systems confirm discussed behavior.

due to the contribution of shear strength, which is non-existent in liquids [30]. The sound velocity of liquid bismuth at ambient pressure (near the starting point of our experiments) is 1.65 km/s [19, 20, 21]) and for solid bcc-bismuth at approximately 0.1 Mbar on the Hugoniot (near the end point of our compression path), the sound velocity is 2.9 - 3.1 km/s [31, 20], suggesting that we should observe a large change in sound velocity upon resolidification. In each experiment, we observe an increase in C_L as the liquid is compressed, followed by a divergent region in C_L as function of

U_p during the transition and finally a decay to a sound speed appropriate for a solid. After resolidification, the obtained C_L have values approximately twice the initial C_L (or somewhat less in terms of the laboratory frame of reference sound velocity $C_e = \rho_o C_L/\rho \approx 0.80 C_L$ [32].) We found no precedence for such divergence in sound velocity during phase transition of compressed materials. Furthermore, we cannot exclude the possibility that voids (caused by densification of bismuth on melting at ambient pressure) or impurities in the sample may have caused the divergence in sound velocities. Further investigations are needed.

We also explored resolidification in water using an experimental set-up similar to that used previously for Bi (Fig. 12c), but with an aluminum container. The particle velocities of the water/LiF interface (Fig. 18) exhibit two wave structures indicative of phase transition. The water-ice transition times scale with sample thickness as ex-

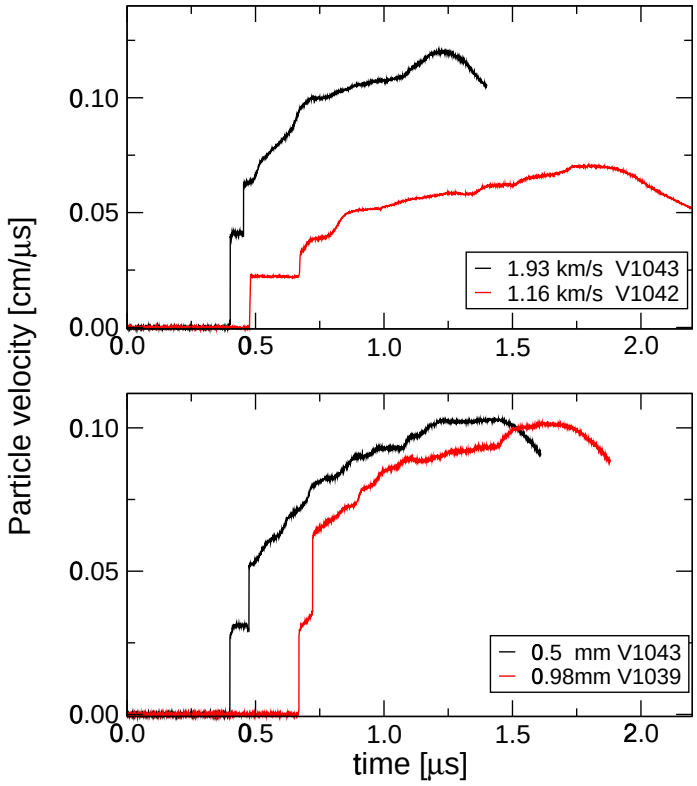

Figure 15: VISAR data taken from only compressed liquid bismuth samples (Fig. 12 (a)) reproducing similar features shown in Fig. 13: (top) impact velocity is varied for a sample thickness 0.7 mm of Bi, and (bottom) thickness of Bi sample is varied for an impactor velocity of 1.6 km/s. The data indicates a sample thickness dependence for the suspected onset of resolidification near 0.08 cm/μs.

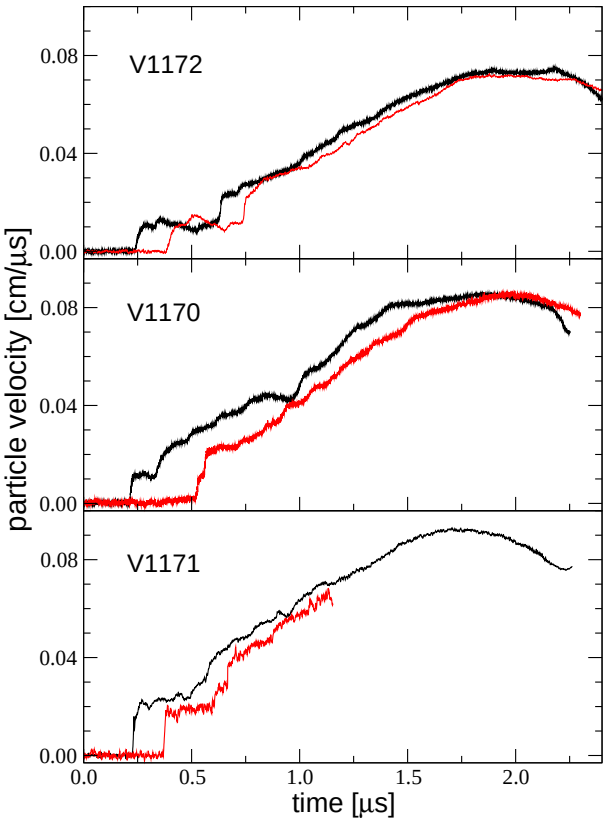

Figure 16: VISAR data taken simultaneously as in Fig. 12 (c). Data V1172 is from 0.5 mm and 0.75 mm thick liquid Bi samples with an impactor velocity 1.2 km/s; V1171 is from 0.75 mm and 1.0 mm with an impactor velocity 1.49 km/s; V1170 is from 0.5 mm and 1.0 mm with an impactor velocity 1.49 km/s. Data from 0.75 mm thick sample (V1172) ends at approximately 1.1 μs due a lost signal.

pected. (Very similar results were obtained in simulations of the $\alpha - \epsilon$ transition in Fe, for instance). Initial simulations of this isentropic-driven experiment indicate that the pressure (about 2.2 GPa) associated with the plateau region (seen at $U_p \approx 200$ m/s) is consistent with the H_2O phase diagram[33]. The plateau regions corresponds to the mixed phase region (path B-C in Fig. 11). Our results are in agreement with previous work on water[34].

Conclusion

Our experiments and simulations indicate that a nearly-isentropic pressure wave can be produced in a two-stage, light-gas gun (with a loading time ranging from ns to μs) by using specifically prescribed density profile impactors. Additionally, with these impactors, we are able to shape the applied compression, and thereby dynamically probe those features of a phase diagram which have some inherent time dependence, such as phase transitions and dynamic response (strength properties, work hardening, fatigue?) along various thermodynamic paths. The hydrodynamic simulations have not only been used to model the experiments, but also have been used as a tool to design the density profile of the impactor for a desired experiment. Currently, this impactor has been applied to liquid-solid phase transitions in bismuth and water. Although we saw the first indications of solidification in bismuth during an isentropic

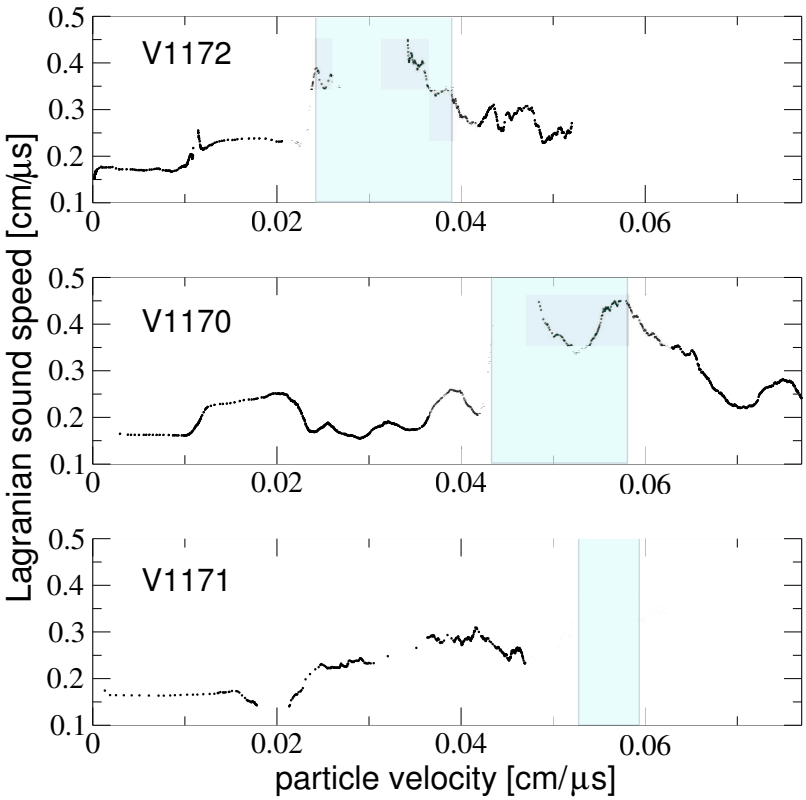

Figure 17: Empirically calculated Lagrangian sound velocity from data in Fig. 16. The blue shaded areas represent regions of particle velocity where the phase transition from liquid Bi to solid Bi is suspected. In this calculation, plateaus in the VISAR data were ignored, e.g. in V1171 near 0.5 μs.

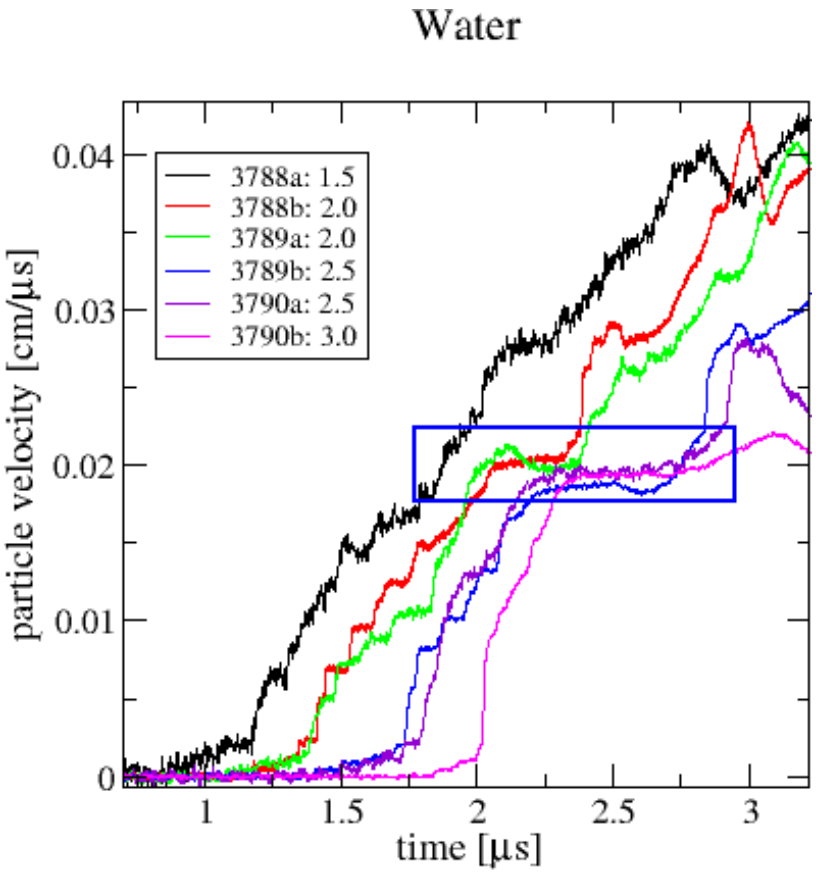

Figure 18: Particle velocities (VISAR) of water/LiF interface. The interface velocities exhibit two-wave structure indicative of phase transition. The transition times increase with sample thickness.

compression, the experiments did not produce consistent results, and further investigation will be needed. Quasi-isentropic compression experiments on water, however, yielded unambiguous signatures of solidification, verifying our general approach and demonstrating the utility of this new capability.

Future Plans

The ability to control details of the time, pressure and temperature scale of a dynamic impact experiment is now a standard part of the experimental repertoire for the lab, and represents the successful transfer of the technology developed in an LDRD-ER directly into the program. Further development of the graded density technology is

being funded directly by the interested programs.

This LDRD-ER also served to heighten awareness of issues relating to time scales and the kinetics of transitions, especially the almost complete lack of experimental data available to our scientists. The laboratory has recognized the need to address these issues - choosing to fund two promising LDRD-ER proposals which grew directly out of this one: one whose focus is on the creation of a new real-time structural diagnostic based on the measurement and interpretation of optical constants and another aimed at measuring the actual time scale of pressure induced solid-solid and solid-liquid phase transformations.

Bibliography

[1] M. Eremets, *High Pressure Experimental Methods*, Oxford University Press, Oxford, 1996.

[2] Y. B. Zel'dovich and Y. P. Raizer, *Physics of Shock Waves and High-Temperature Hydrodynamic Phenomena*. (Academic Press, New York, 1967).

[3] Duvall, G. E. & Graham, R. A. Phase transitions under shock-wave loading. *Rev. Mod. Phys.***49**, 523-579 (1977).

[4] C. A. Hall, *Phys. Plasma* **7**, 2069 (2000).

[5] C. A. Hall et al., *Rev. Sci. Instru.* **72**, 3587 (2001).

[6] Reisman, D. B., et al. Magnetically driven isentropic compression experiments on the Z accelerator. *J. Appl. Phys.* **89**, 1625-1633 (2001).

[7] J. Edwards, *Phys. Rev. Lett.* (submitted) (2003).

[8] Q. Shen et al., *Acta Phys. Sinica*, **51**, 1759 (2002).

[9] L. M. Barker, High-pressure Quasi-isentropic Impact Experiments. *Shock Waves Cond. Matt.* J. R. Asay, R. A. Graham and G. K. Straub, (eds.) (Elsevier Sci. Pub., Amsterdam)(1984).

[10] Chhabildas, L. C., Asay, J. R. & Barker, L. M. *Shear Strength of Tungsten Under Shock- and Quasi-Isentropic Loading to 250 GPa*, **SAND88–0306** Sandia Nat. Lab., Albuquerque, New Mexico(April 1988).

[11] Hoover, W. G. Structure of a shock-wave front in a liquid. *Phys. Rev. Lett.***42**, 1531-1534 (1979).

[12] Steinberg, D. J., Cochran, S. G. & Guinan, M. W. A constituitive model for metals applicable at high-strain rate. *J. Appl. Phys.* **51**, 1498-1504 (1980).

[13] The Velocity Interferometer System for Any Reflector (VISAR) measures the change in the Doppler shift of the reflected light off a moving surface. The VISAR used in this experiment has sub-nanosecond temporal resolution. See L. M. Barker and R. E. Hollenbach, *J. Appl. Phys.* **43**, 4669 (1972).

[14] Follansbee P. S., in *Impact Loading and Dynamic Behavior of Materials*, ed. C. Y. Chiem, H. D. Kunze and L. W. Meyer, Springer-Verlag, Berlin, 1988

[15] M. V. Patel and F. H. Streitz, in preparation.

[16] need reference here for HE experiments

[17] C. Mabire and P. L. Héreil, Shock Induced Polymorphic Transition and Melting of Tin, *Shock Comp. Cond. Matt.* M. D. Furnish, L. C. Chhabildas, and R. S. Hixson, (eds.) (AIP Conf. Proc., Melville, New York)(1999) pp. 93-96.

[18] J. H. Nguyen, D. Orlikowski, F. H. Streitz, N. C. Holmes and J. A. Moriarty, Specifically prescribed dynamic thermodynamic paths and resolidification experiments, *Shock Comp. Cond. Matt.* M. D. Furnish, L. C. Chhabildas, and R. S. Hixson, (eds.) (AIP Conf. Proc., Melville, New York)(2004) pp. xx-xx.

[19] Pashuk, E. G. & Pashaev, B. P Ultrasonic velocity in metallic melts in a wide temperature range. *High Temp.* **18**, 256-260 (1980).

[20] Péllisier, J. L. & Wetta, N. A model-potential approach for bismuth (I): densification and melting curve calculation. *Physica A* **289**, 459-478 (2001).

[21] Wetta, N. & Péllisier, J. L. A model-potential approach for bismuth (II): behaviour under shock loading. *Physica A* **289**, 479-497 (2001).

[22] A. Sharma *et al.*, *Science* **297**, 5580 (2002).

[23] Andrews, D. J. Calculation of mixed phases in continuum mechanics. *J. Comput. Phys.* **7**, 310 (1971).

[24] Hayes, D. B. Wave propagation in a condensed medium with N transforming phases: application to solid-I-solid-II-liquid bismuth. *J. Appl. Phys.* **46**, 3438 (1975).

[25] Boettger, J. C. & Wallace, D. C. Metastability and dynamics of the shock-induced phase transition in iron. *Phys. Rev. B* **55**, 2840 (1997).

[26] Kadau, K., Germann, T. C., Lomdahl, P. S., Holian, B. L. Microscopic view of structural phase transitions induced by shock waves. *Science* **296**, 1681 (2002).

[27] Steinberg, D. J. & Lund, C. M. A constitutive model for strain rates from 10^{-4} to 10^6 s−1 . *J. Appl. Phys.* **65**, 1528-1533 (1989).

[28] The gradual reduction in U_p can also be attributed to the possible existence of many solid phases in that region of the phase diagram.

[29] The Lagrangian sound velocity is calculated as $\Delta h/\Delta t$, where Δh is the initial difference between sample thicknesses and Δt is the difference in time between the two samples at constant U_p [6]. In determining this, we ignored larger plateaus in the U_p, e.g. at 0.5 μs in V1171, which is due to the impactor. As the system approaches the melt line, a divergent region is revealed in C_L as function of U_p. The initial C_L is equal to Eulerian sound velocity C_e, since $C_L = \rho C_e/\rho_o$ where ρ_o is ambient density.

[30] In metals such as 2024 aluminum, molybdenum, tantalum and iron, the percent change in sound velocities on shock melting ranges from 6% to 14% (or about 0.6 km/s to 1.5 km/s in sound velocity) [35, 58, 59, 60]. These experiments were carried out at megabar pressures. However, this gives an estimate of the expected increase in sound velocity for the liquid to solid Bi phase transition.

[31] Pavlovskii, M. N. & Komissarov, V. V Peculiarities of the phase transformation of bismuth in a rarefraction wave. *Sov. Phys. JETP* **56**, 1244-1246 (1982).

[32] The decreasing C_L after resolidification may be due to reflection waves. A rarefraction wave from the Bi/LiF interface transverses the Bi sample opposite to the applied pressure wave, thus interacting with not only the phase transition boundary that moves through the sample, but also with the Cu/Bi interface as well. This issue can be further investigated with sample-size dependent experiments and hydrodynamic simulations to minimize the effect of the reflection waves.

[33] Lobban, C., Finney, J. L., & Kuhs, W. F. The structure of a new phase of ice. *Nature* **391**, 268-270 (1998).

[34] D.H. Dolan and Y.M. Gupta, Chem. Phys. Lett. **374**, 608-621 (2003).

[35] J. H. Nguyen and N. C. Holmes, *Nature* **427**, 339 (2004).

[36] W. B. Hubbard *et al.*, *Phys. of Plasmas* **4**, 2011 (1997).

[37] H. Herberhold *et al.*, *J. Mol. Biol.* **330**, 1153 (2003).

[38] P. Ehrenfreund*et al.*, *Rep. Prog. Phys.* **65**, 1427 (2002).

[39] H. Cynn, J. E. Klepeis, C. S. Yoo and D. A. Young, *Phys. Rev. Lett.* **88**, 135701 (2002).

[40] V. V. Struzhkin *et al.*, *Science* **298** 1213 (2002).

[41] M. I. Eremets, V. V. Struzhkin, H. K. Mao, and R. J. Hemley, *Science* **293** 272 (2001).

[42] V. V. Struzhkin, R. J. Hemley, H. K. Mao, and Y. A. Timofeev, *Nature* **390** 382 (1997).

[43] S. C. Schmidt, D. S. Moore, D. Schiferl, and J. W. Shaner, *Phys. Rev. Lett.* **50**, 661 (1983).

[44] N. C. Holmes, W. J. Nellis, W. B. Graham and G. E. Walrafen, *Phys. Rev. Lett.* **55**, 2433 (1985).

[45] F. P. Bundy *et al.*, *Carbon* **34**, 141 (1996).

[46] V. Iota, C. S. Yoo, and H. Cynn, *Science* **283**, 1510 (1999).

[47] W. J. Nellis, S. T. Weir, and A. C. Mitchell, *Phys. Rev. B* **59**, 3434 (1999).

[48] A. L. Ruoff, H. Xia, and Y. Vohra, *Rev. Sci. Instrum.* **61**, 3830-3 (1990).

[49] M. Knudson *et al.*, *J. Appl. Phys.* **94**, 4420 (2003).

[50] D. Batani *et al.*, *Eur. Phys. J. D* **23**, 99-107 (2003).

[51] R. Cauble *et al.*, *Phys. Rev. Lett.* **70**, 2102 (1993).

[52] P. W. Bridgman, *Proc. Am, Acad. Arts Sci.* **81** 167-251, (1952).

[53] The Hugoniot is the locus of thermodynamic states which can be reached from a given initial state by passage of a shock. A Hugoniot is thus not a thermodynamic path that maintains local equilibrium—the system moves discontinuously through phase space to some point on the Hugoniot.

[54] Since the sound speed, $c^2 = dP/d\rho|_S$, is an increasing function of pressure, a compression wave eventually stiffens into a propagating shock wave for a thick target. Hence, the steeper the initial pressure ramp, the thinner the material must be before the wave becomes a shock. This problem is worse in materials with large atomic number.

[55] Nellis, W. J., Weir, S. T. & Mitchell, A. C. Metallization and Electrical Conductivity of Hydrogen in Jupiter. *Science* **273**, 936 (1996).

[56] Furnish, M. D., et al. Using the Saturn Accelerator for Isentropic Compression Experiments,**SAND2001-3773** Sandia Nat. Lab., Albuquerque, New Mexico (Dec. 2001).

[57] Tipton, R., Managan, R. & Amala, P. *CALE users manual*(Lawrence Livermore National Laboratory, Livermore California)(2002).

[58] Hixson, R. S., Boness, D. A., Shane, J. W., Moriarty, J. A., Acoustic velocities and phase transitions in molybdenum under strong shock compression, *Phys. Rev. Lett.* **62**, 637 (1989).

[59] Brown, J. M. and Shaner, J. W., in *Shock Compression of Condensed Matter - 1983*, edited by Asay, J. R., Graham, R. A., and Straub, G. K., Shock Waves in Condensed Matter - 1983, (Amsterdam 1984), pp. 91-94.

[60] McQueen, R. G., Fritz, J. N., Morris, C. E., in *Shock Compression of Condensed Matter - 1983*, edited by Asay, J. R., Graham, R. A., and Straub, G. K., Shock Waves in Condensed Matter - 1983, (Amsterdam 1984), pp. 95-98.

[61] Moriarty, J. A., et al., Quantum-based atomistic simulation of materials properties in transition metals. *J. Phys. Condens. Matter* **14**, 2825-2857 (2002).

[62] Hayes, D., Vorthman, J., & Fritz, J. Backward integration of a VISAR Record: free surface to the spall plane **LA-13830-MS** Los Alamos Nat. Lab. Los Alamos, New Mexico (May, 2001).

[63] Aidun, J. B. & Gupta, Y. M. Analysis of lagrangian gauge measurements of simple and non-simple plane waves. *J. Appl. Phys.* **69**, 6998 (1991).